Jacobeit, J., A. Dünkeloh & E. Hertig (2007): Mediterranean rainfall changes and their couses. In: Lozán, J. L., H. Grassl, P. Hupfer, L. Menzel & C.-D. Schönwiese. Global Change: Enough water for all? Wissenschaftliche Auswertungen, Hamburg. 384 S. Online: www.klima-warnsignale.uni-hamburg.de

3.1.8 Mediterranean rainfall changes and their causes

JUNCUDUS JACOBEIT, ARMIN DÜNKELOH & ELKE HERTIG

SUMMARY: *Based on a revised version of the CRU (Norwich) gridded monthly rainfall data, trends in Mediterranean precipitation for the 1951–2000 period are calculated on a seasonal scale. The most important characteristic is the widespread rainfall decrease during the winter half-year which is linked to particular changes in atmospheric circulation patterns identified by canonical correlation analyses: a shift to preferred positive modes of the NAO-linked Mediterranean Oscillation since the 1980s, a weakening of the central Mediterranean trough since the late 1980s, and a modal change since the 1970s implying increased pressure in the Mediterranean area. Statistical downscaling assessments for enhanced greenhouse conditions at the end of the 21st century indicate some further developments: rainfall increases in high winter and decreases in spring and autumn for western and northern Mediterranean regions, but mainly negative changes throughout the rainy period for southern and eastern regions.*

With respect to rainfall changes those regions are focussed in particular which are characterised by difficult conditions of water budget and water supply or by indications for an unfavourable future development in precipitation. Both is true for the Mediterranean region and has generated a huge amount of scientific literature related to these issues (see corresponding reviews in DÜNKELOH & JACOBEIT 2003, HERTIG 2004, TRIGO et al. 2006). This chapter will look at rainfall trends of the last five decades and will point to relationships with atmospheric circulation changes. Finally, an outlook is given for the late decades of the 21st century under conditions of an enhanced man-made greenhouse warming.

Precipitation trends 1951–2000

Calculations are based on the gridded data set from the Climatic Research Unit (CRU) in Norwich (NEW et al. 2000) revised and updated by the Potsdam-Institute for Climate Impact Research (PIK). The monthly station-based data are released with a 0.5°×0.5° resolution, inhomogeneities identified by moving t-tests have been removed in this revised PIK version of the data set (OESTERLE et al. 2003); furthermore, PIK has also performed some assimilation to station data of the Global Precipitation Climatology Centre (GPCC).

Fig. 3.1.8-1a, covering the whole winter half-year from October to March, reveals the predominating rainfall decreases during the last 50 years with a maximum around 250 mm in the area of NW-Greece/Albania. However, this trend was preceded by a long-term rainfall increase (LUTERBACHER et al. 2006) which even peaked not before the 1960s. Remarkably, a larger area does not join this predominant rainfall decrease according to *Fig. 3.1.8-1a* showing a moderate increase which proves to be insignificant but consistent with circulation dynamics (see below). This area includes southern Israel and the neighbouring coastal region of North Africa up to Libya. Another pattern is indicated for the transitional period of April and May (*Fig. 3.1.8-1b*): rainfall increases, partly even at the 95% confidence level, within the Iberian peninsula (except of its south-eastern border), in northern parts of the central Mediterranean area and eastward of the Syrte region, in contrast to that, however, rainfall reductions around the south-western Mediterranean area and in the Levant region. Of course, the contribution of this 2-month season to the entire precipitation is much lower than for the 6-month season discussed before. For the summer time with generally low amounts of rainfall, there are hardly significant long-term trends due to the high variability of occasional shower events. The autumn months from September to November depict again rainfall reductions in the south-western Mediterranean area and in the Aegean region, but also some regional increases in western Iberia, in the northern Mediterranean area and in the coastal region of southern Turkey (JACOBEIT 2000). These seasonal increases, however, are not able to compensate for the dominating rainfall decreases during the whole winter half-year (*Fig. 3.1.8-1a*).

Relationships with atmospheric circulation changes

Analysing the Mediterranean rainfall grids by means of canonical correlation analysis in conjunction with North-Atlantic-European geopotential height fields (only shown for the 500 hPa level based on NCEP/NCAR reanalyses data), we get pairs of patterns for the large-scale atmospheric circulation and the Mediterranean precipitation being optimally correlated and representing the essential relationships between these two quantities. *Fig. 3.1.8-2* gives an example of two pairs of patterns for the winter half-year, complete results may be found in DÜNKELOH & JACOBEIT (2003), referring to the winter season also in JACOBEIT & DÜNKELOH (2003) and in XOPLAKI et al. (2004). The first pair of canonical patterns (W-CCP1) reveals a particular contrast between the western-central and the (south-) eastern Mediterranean

Jucundus.Jacobeit@geo.uni-Augsburg.de

area which has also been denoted as »Mediterranean Oscillation« (Conte et al. 1989). Its positive mode (shown in *Fig. 3.1.8-2*) with positive (negative) deviations of geopotential heights in the western (eastern) parts leads to below- (above-) normal winter rainfall in these regions, with negative time coefficients this distribution will be inverted (negative mode of W-CCP1).

As may be seen from the highly correlated (r = 0,92) time coefficients of W-CCP1 in *Fig. 3.1.8-2*, the Mediterranean Oscillation has underwent a significant change (0,1% error probability) during the last 50 years: until 1970 there was still a predominance of the negative mode, whereas since the 1980s preferably the positive mode occurs. This circulation change is partly responsible for the negative rainfall trends in the western-central Mediterranean area (*Fig. 3.1.8-1a*), at the same time it offers a dynamic explanation for the opposite development in the south-eastern region. The Mediterranean Oscillation itself is further linked to large-scale dynamics: it is correlated with the Arctic Oscillation AO (r = 0,60) as well as with the North Atlantic Oscillation NAO (r = 0,72). Thus, as regional manifestation of hemispheric-scale circulation regimes, it puts the observed rainfall trends in the Mediterranean area into perspective of large-scale dynamics which include in particular the well-known increase in the winter NAO-index during the last decades.

But there are further important forcings as may be seen from the second pair of canonical patterns (W-CCP2) in *Fig. 3.1.8-2*: it has particular importance for the north-eastern part of the Mediterranean area and may be called »Mediterranean Meridional Circulation« pattern in accordance with the arrangement of its pressure anomaly centres. Its time coefficients reveal a significant turn at the end of the 1980s from preferably positive modes to a

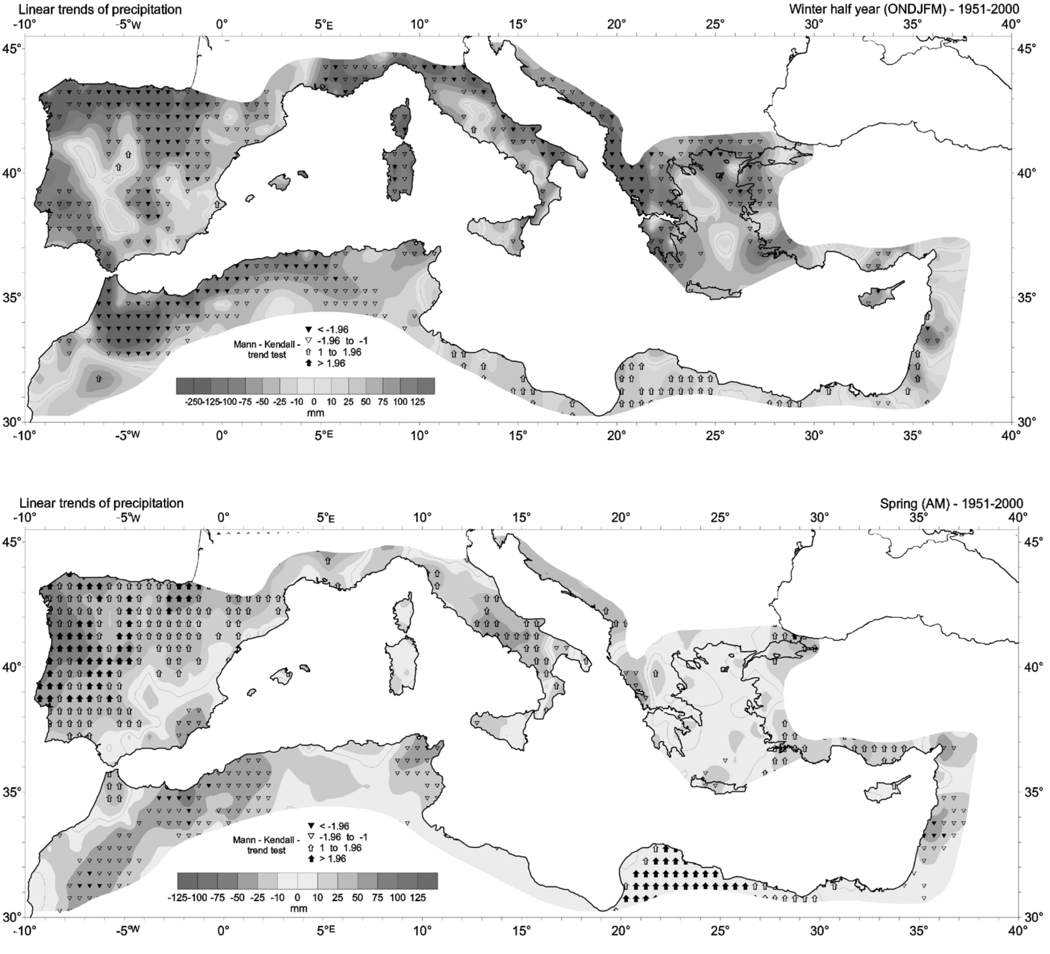

Fig. 3.1.8-1: Rainfall trends 1951–2000 based on the CRU/PIK data set. Black symbols indicate significance at the 95% level (for light symbols only around 68%). *Upper part (a)*: October to March; *Lower part (b)*: April to May.

distinct predominance of the negative mode, i.e. the most recent period is characterised by inverted deviations compared to those shown for W-CCP2 in *Fig. 3.1.8-2*. This weakening of the central Mediterranean trough implies positive pressure anomalies and corresponding negative rainfall deviations for the central to eastern Mediterranean area as well as the opposite for the western regions. Superimposed with the changes of the Mediterranean Oscillation (W-CCP1), the largest deficits in precipitation should occur in parts of the central-eastern Mediterranean area. This is in fact true for the region around NW Greece and Albania, however not so widespread as to be expected from *Fig. 3.1.8-2*. This is due to a further pair of canonical patterns (not shown) which contributes to a pressure rise especially at the western and eastern borders of the Mediterranean area since the 1970s (DÜNKELOH & JACOBEIT 2003). These conditions further imply that the above-mentioned south-eastern rainfall increase remains rather weak on the whole.

The rainfall trends of spring (*Fig. 3.1.8-1b*) are also related to circulation changes with particular importance of a 3-core pattern (positive pressure deviations in the south-western and the eastern region, negative ones from the British Isles towards the central Mediterranean area). However, lower percentages of the total rainfall variance are accounted for, and the correspondence with large-scale circulation dynamics is less distinct than in winter. Generally, for all seasons it remains still open whether the observed trends and shifts are primarily reflecting natural variability on decadal time scales or whether they are due in large parts to man-made climate changes. Therefore we will look at possible future rainfall conditions being assessed for assumptions of an enhanced man-made greenhouse warming.

Rainfall changes due to further enhanced man-made greenhouse warming

For these assessments after HERTIG (2004), statistical downscaling techniques (in this case based on canonical correlation analyses) have been used including as a first step the derivation of observation-based relationships between large-scale predictors (in this case geopotential height and specific humidity grids for the North-Atlantic-European region) and small-scale predictands (in this case the Mediterranean CRU/PIK rainfall grids). Statistical models from 10 different calibration periods have passed a particular cross validation, the accepted ones have been used in a subsequent step to predict Mediterranean rainfall from large-scale predictors of various numerical climate model simulations assuming further enhanced man-made greenhouse warming (HERTIG & JACOBEIT 2006). Results from *Fig. 3.1.8-3* are based on predictors from a simulation run with the coupled Hamburg climate model ECHAM4/OPYC3 according to the emission scenario B2 which assumes a medium level of economic development and a continuously increasing population (NAKICENOVIC & SWART 2000). *Fig. 3.1.8-3* compares, for overlapping 2-month seasons, statistically estimated rainfall amounts of the two 30-year periods 2071–2100 and 1990–2019. Main results which are discussed in more detail by HERTIG (2004) are the following:

During autumn (Oct.–Nov.) enhanced greenhouse warming leads preferably to reduced rainfall except of the eastern border of Spain and along the Syrte coast. During central winter (Dec.–Jan.), however, distinct increases in the western and northern parts, less marked decreases in the southern and eastern parts occur. Some times later (Feb./Mar.) the area with decreasing precipitation has been extended again, increasing rainfall only occurs in the outermost northern and western parts. Spring (Apr./May) is generally characterised by reduced rainfall. Thus, both transitional seasons are dominated by decreasing precipitation. In a regional context – and this is also true for winter – especially the southern and the eastern regions are affected by a further reduction of rainfall.

However, many uncertainties of such assessments have to be considered. At first, statistical significance in terms of the signal-to-noise ratio is reached for only few of the estimated rainfall changes due to the high rainfall variability in the Mediterranean area. Furthermore, results differ somewhat in dependence of the particular emission scenarios, the numerical model predictors, and the downscaling techniques. For example, results from dynamical downscaling by regional climate models (e.g. GIORGI et al. 2004) indicate a more northern transition in winter between rainfall increase to the north and rainfall decrease to the south compared to *Fig. 3.1.8-3*. Nevertheless, conditional assessments of future changes may give an idea of latent risks which do exist in view of 30–50% reductions in rainfall indicated just for regions being already quite dry during recent times. Another confirmation might be given by the fact that main results of future projections are increasingly converging also in comparison with earlier approaches to this issue (e.g. JACOBEIT 1996).

Conclusions

Comparing recent trends with future projections, no complete correspondence is given: thus, for the western and northern Mediterranean area, we now observe decreasing rainfall during winter, but also some increasing rainfall during the transitional seasons, whereas an opposite change is indicated for the late 21st century (some increase in parts of winter, reductions before and after that). The major problem areas, however, are located in

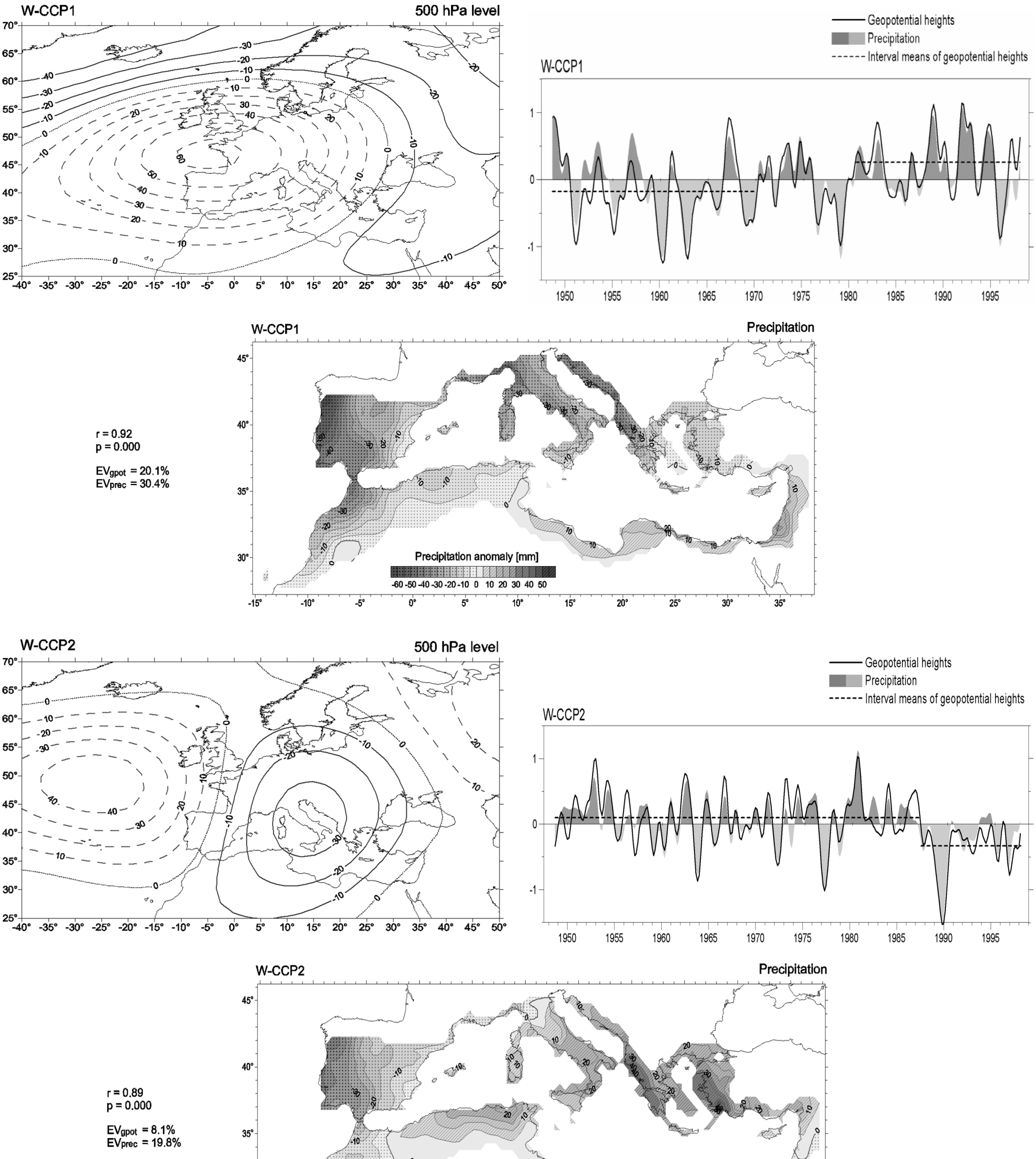

Fig. 3.1.8-2: First and second canonical correlation patterns (W-CCP1, W-CCP2) for geopotential heights (500 hPa level) and Mediterranean precipitation as well as low-pass filtered time coefficients resulting from an analysis for Oct.-Mar. 1948–1998. r: canonical correlation coefficient; p: error probability; $\mathbf{EV}_{gpot}$: *explained variance for geopotential heights*; $\mathbf{EV}_{prec}$: *explained variance for precipitation*. Dashed lines for the time coefficients indicate mean values for particular intervals differing significantly at the 0,1% error probability (after Dünkeloh & Jacobeit 2003).

the southern and the eastern parts being already affected by rainfall reductions – except of a limited south-eastern region with a moderate increase – and moving towards an enhanced greenhouse future which will probably include further rainfall reductions throughout the entire rainy period♦

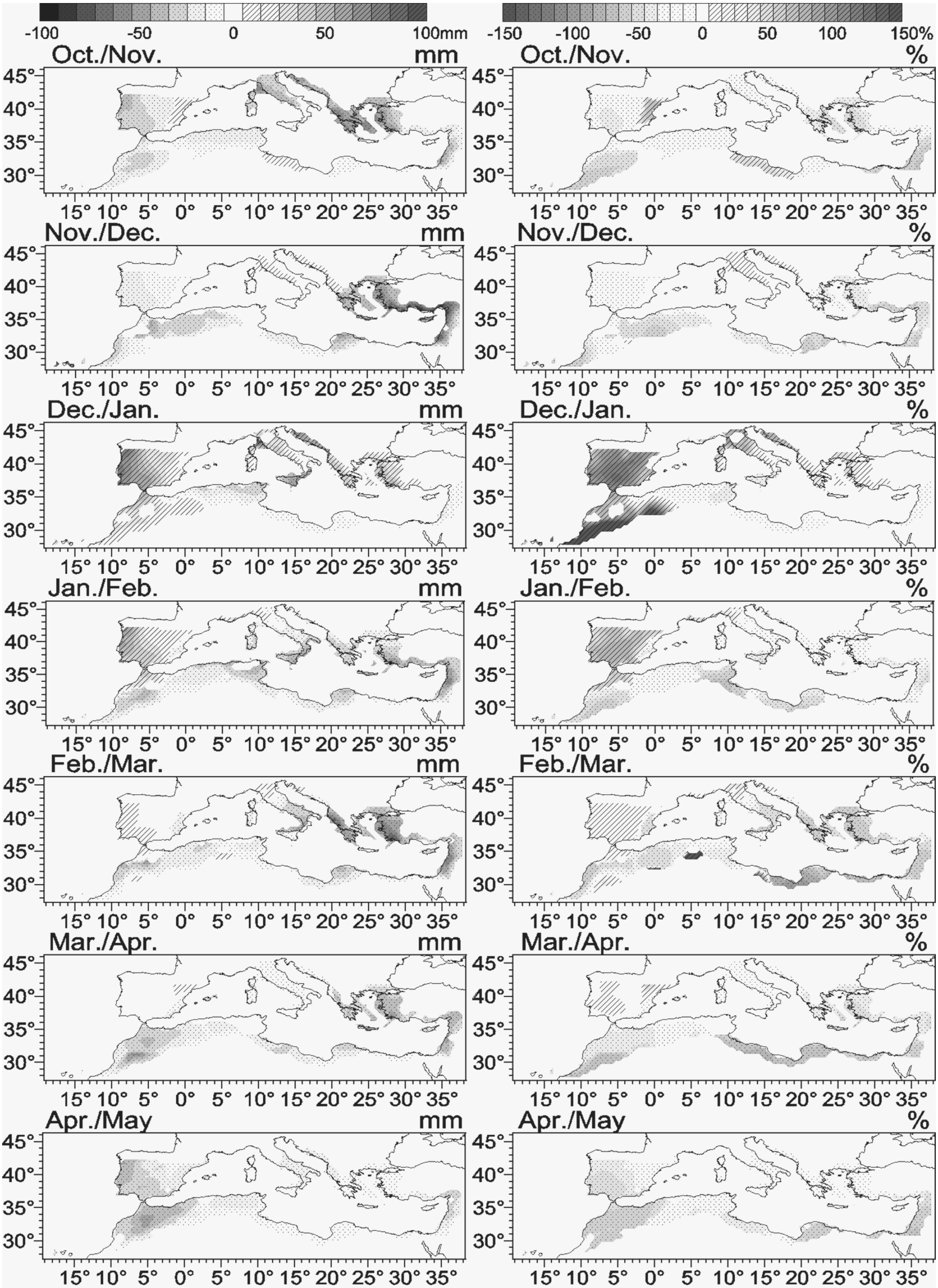

Fig. 3.1.8-3: Estimated rainfall changes 2071–2100 compared to 1990–2019. Left: differences in mm between these periods; right: differences in % of the earlier values. Statistical downscaling by canonical correlation analyses using large-scale ECHAM4/OPYC3 predictors (see text) according to the emission scenario B2 (after HERTIG 2004).